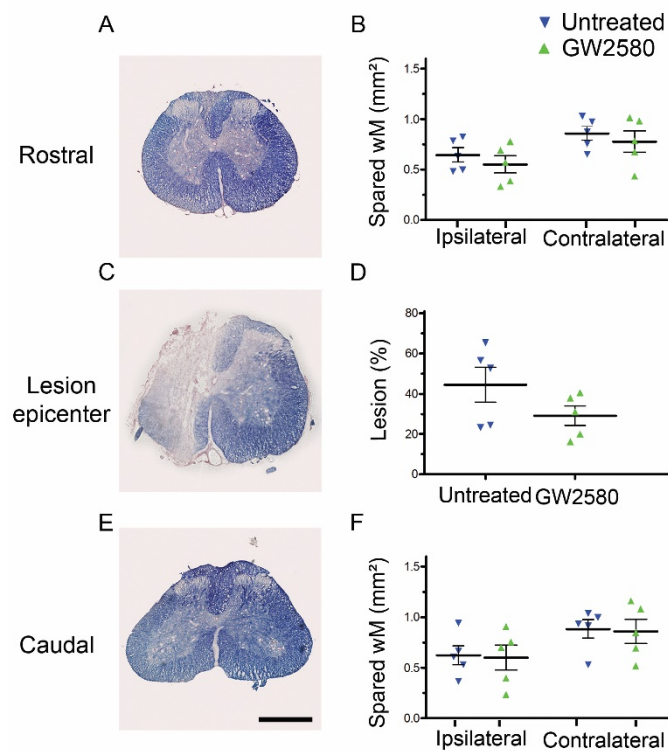


Supplementary data

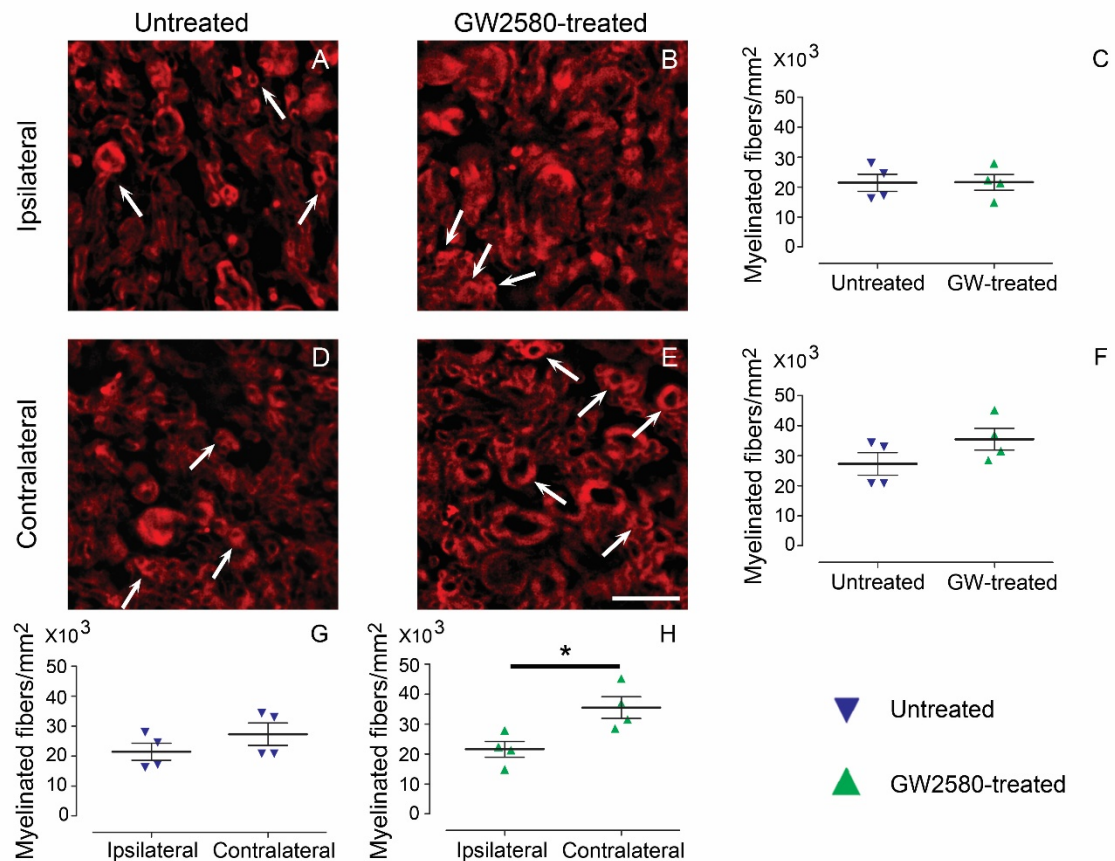
Inhibiting microglia proliferation after spinal cord injury improves recovery in mice and nonhuman primates

Gaëtan Poulen, Emilie Aloy, Claire M. Bringuier, Nadine Mestre-Francés, Emaëlle V.F. Artus, Maïda Cardoso, Jean-Christophe Perez, Christophe Goze-Bac, Hassan Boukhaddaoui, Nicolas Lonjon, Yannick N. Gerber and Florence E. Perrin



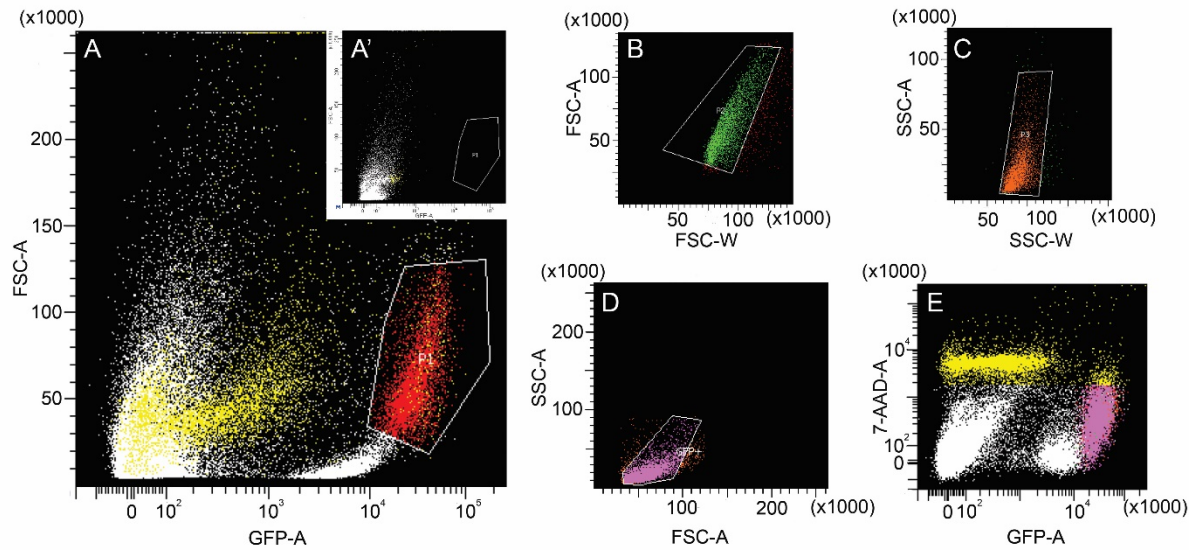
Supplementary Figure 1: Transient CSF1R blockade after lateral spinal cord hemisection in nonhuman primates modifies lesion extension

Bright-field micrographs displaying Luxol fast blue and neutral red stained axial sections rostral (A) within (C), and caudal (E) to the lesion site at 3 months after SCI in a GW2580-treated nonhuman primate. Luxol-based quantifications of the spared white matter (WM) rostral (B) and caudal (F) to the lesion site as well as the percentage of damaged tissue at the epicenter (D). Scale bar: 600 μ m. In all graphs, results for untreated nonhuman primates are in blue and GW2580-treated in green. Each point for a given animal represents the mean of 16 slices (B&F) Data are mean \pm SEM. Number of injured *Microcebus murinus*: untreated n=5 and GW2580-treated for 2 weeks n=5.



Supplementary Figure 2 : Transient CSF1R blockade after lateral spinal cord hemisection in nonhuman primates modifies outcomes on myelinated fibers

Photographs of fluoromyelin staining of untreated (A&D) and GW2580-treated (B&E) *Microcebus murinus*. Pictures of axial section of the thoracic spinal cord taken in the lateral *funiculus* 1.68 mm caudal to the lesion epicenter on the ipsilateral (A&B) and contralateral (D&E) sides of the lesion. Quantification of intact myelin sheaths on the ipsilateral (C) and contralateral (F) sides of the lesion in untreated and GW2580-treated animals 3 months after SCI. Intact myelin sheaths quantification on the ipsilateral and contralateral sides of the lesion in untreated (G) and GW2580-treated (H) animals. In all graphs, results for untreated nonhuman primates are in blue and GW2580-treated in green. Four animals selected randomly in each group (untreated and GW2580-treated) and 2 pictures (ipsilateral and contralateral) were quantified per lemur. Data are mean ± SEM per group. Student's unpaired t-test, *p < 0.05. Scale bars: A-D, 10µm. Arrows (A&D and B&E) point to intact myelin sheaths.



Supplementary Figure 3: gating strategy for FACS

Representative flow cytometry from injured CX3CR1^{+/-GFP} male mice displaying eGFP^{high} expressing microglia designed as P1 (A) as compared to FACS profile of injured “none GFP” mice (A’). Gating strategy based on doublet exclusion (B) and morphology (C) for selected eGFP^{high} expressing cell population. Flow cytometry profile displaying sorted cells, designed as “GFP+”, that correspond to the eGFP^{high}-expressing microglia further analyzed using transcriptomic (D) excluding dead cells stained with 7AAD (E, appear in yellow). FSC: Forward Scatter; SSC: Size Scatter; A: Area; W: Width.

Supplementary Table 1. Database of differential expression comparison of microglia from GW2580-treated and untreated mice at 1 week after spinal cord hemisection. p-value with FDR≤0.05 and FC≥2.

Gene	Description	GO Process	Fold Change	p-value with FDR
<i>Cd38</i>	CD38 antigen	Negative regulation of neuron projection	-7.71	0.0024
<i>Cd40</i>	CD40 antigen	Immune process	-3.48	0.0124
<i>Cxcl13</i>	Chemokine (C-X-C motif) ligand 13	Immune process	-3.34	0.0214
<i>Pf4</i>	Platelet factor 4	Inflammatory response	-3.3	0.0155
<i>Emilin2</i>	Elastin microfibril interfacier 2		-3.12	0.0057
<i>Lyz1</i>	Lysozyme 1	Defense response to bacterium	-2.89	0.0402
<i>Msr1</i>	Macrophage scavenger receptor 1	Positive regulation of macrophage derived foam cell differentiation	-2.82	0.0024
<i>Fn1</i>	Fibronectin 1	Positive regulation of cell proliferation regulation	-2.80	0.0087
<i>Cspg4</i>	Chondroitin sulfate proteoglycan 4	Cell population proliferation, glial cell migration	-2.74	0.0107
<i>Adm</i>	Adrenomedullin	Positive regulation of cell proliferation regulation	-2.59	0.0327
<i>Cybb</i>	Cytochrome b-245. beta polypeptide	Inflammatory response	-2.27	0.0024
<i>Pltp</i>	Phospholipid transfer protein	Lipid metabolic process	-2.27	0.0201
<i>Gpx3</i>	Glutathione peroxidase 3	Response to oxidative stress	-2.26	0.0057
<i>Lyz2</i>	Lysozyme 2	Killing of cells of other organism	-2.12	0.0134
<i>Itsn1</i>	Intersectin 1 (SH3 domain protein 1A)	Brain development	-2.07	0.0407
<i>Gpnmb</i>	Glycoprotein (transmembrane) nmb	Positive regulation of cell migration	-2.07	0.0051
<i>Kcnk12</i>	Potassium channel. subfamily K. member 12	Potassium ion transmembrane transport	2.06	0.0377
<i>Srpk3</i>	Serine/arginine-rich protein specific kinase 3	Cell differentiation	2.08	0.0104
<i>Sdk1</i>	Sidekick cell adhesion molecule 1	Cell adhesion	2.32	0.0191

Supplementary Table 2. Enrichment analysis in the comparison of microglia from GW2580-treated and untreated mice at 1 week after spinal cord hemisection. p-value with FDR≤0.05 and FC≥2.

Rank	Molecular function	p-value with FDR	Genes in data vs total genes in the pathway	Genes
1	CXCR3 chemokine receptor binding	7.314E-4	2/5	<i>Cxcl13, Pf4</i>
2	Heparin binding	1.150E-3	4/221	<i>Gpnmb (Osteoactivin), fibronectin, Cxcl13, Pf4</i>
3	Lysozyme activity	6.219E-19	2/13	<i>Lyz1, Lyz2</i>

Rank	Processes	p-value/FDR	Genes in data vs total genes in the pathway	Genes
1	Inflammatory response	5.588E-05	8/874	<i>Adrenomedullin, Cd40, Cspg4, fibronectin, Cxcl13, Pf4, Cybb, Lysozym</i>
2	Regulation of angiogenesis	1.487E-04	6/484	<i>Adrenomedullin, Cd40, Cxcl13, Pf4, Cybb, Gpnmb (Osteoactivin)</i>
3	Regulation of developmental process	1.487E-04	12/3978	<i>Adrenomedullin, Cd38, Cd40, Cspg4, fibronectin, Cxcl13, Cybb, Gpnmb (Osteoactivin), Gpx, Intersectin, Msr1, Intersectin</i>
4	Response to other organism	1.487E-04	10/2427	<i>Adrenomedullin, Cd40, fibronectin, Cxcl13, Cybb, Gpx, Gpx3, Lysozyme, Lyz2, Pf4</i>
5	Response to external biotic stimulus	1.487E-04	10/2431	<i>Adrenomedullin, Cd40, fibronectin, Cxcl13, Cybb, Gpx, Gpx3, Lysozyme, Lyz2, Pf4</i>